

Chiral non-Abelian vortex molecules in dense QCD

Sven Bjarke Gudnason¹, Muneto Nitta^{2,3}

¹*Institute of Contemporary Mathematics, School of Mathematics and Statistics, Henan University, Kaifeng, Henan 475004, P. R. China*

²*Department of Physics & Research and Education Center for Natural Sciences, Keio University, Hiyoshi 4-1-1, Yokohama, Kanagawa 223-8521, Japan*

³*International Institute for Sustainability with Knotted Chiral Meta Matter (SKCM²), Hiroshima University, 1-3-2 Kagamiyama, Higashi-Hiroshima, Hiroshima 739-8511, Japan*

E-mail: [gudnason\(at\)henu.edu.cn](mailto:gudnason@henu.edu.cn), [nitta\(at\)phys-h.keio.ac.jp](mailto:nitta@phys-h.keio.ac.jp)

ABSTRACT: The color-flavor locked phase of high density QCD admits non-Abelian vortices, that are superfluid vortices with confined color-magnetic fluxes. Vortex solutions were thus far constructed in an axially symmetric Ansatz with common vortex winding in the left- and right-handed diquark condensates. In this paper, we explore vortex solutions without any Ansatz. In addition to axially symmetric configurations known before, we find that the axial symmetry is broken in certain parameter regions; in one case a single vortex is split into two chiral non-Abelian vortices, i.e. vortices with winding only in the left or right-handed diquark condensate, and they are connected by one or two domain walls forming a non-Abelian vortex molecule. In the other case, a chiral non-Abelian vortex molecule is confined inside a domain wall elongated to spatial infinity.

Contents

1	Introduction	1
2	Color-flavor-locked phase of 3-flavor dense QCD	3
2.1	Ginzburg-Landau model for the color-flavor locked phase	3
2.2	First variation	5
2.3	Ground states	6
3	Chiral vortex molecules	7
3.1	Vortex Ansätze for initial conditions	8
3.2	Diagonal matrices	9
3.3	Numerical method	9
3.4	Numerical results	10
4	Conclusion and outlook	18

1 Introduction

Exploring states of matter in extreme conditions is an important problem in modern physics. In particular, nuclear and quark matter in extreme conditions such as high density, strong magnetic field, and rapid rotation are considered to be pivotal for a full understanding of the interior of compact stars such as neutron stars. The quark matter described by quantum chromodynamics (QCD) at high densities and low temperatures is expected to exhibit color superconductivity as well as superfluidity [1]. In the limit of extremely high density, a phase with three-flavor symmetric matter called the color-flavor locked (CFL) phase is realized [2], while the two-flavor superconducting (2SC) phase [3, 4] is also proposed for the intermediate-density region of the QCD phase diagram. In metallic superconductors and superfluids, quantum vortices or magnetic flux tubes play significant roles in color-superconducting quark matter, as reviewed in ref. [5]. In the CFL phase, the most fundamental stable vortices are non-Abelian vortices carrying color-magnetic fluxes and $1/3$ superfluid circulation [5–11].¹ Superfluid vortices without fluxes called Abelian vortices [28, 29] are dynamically unstable to decay into three non-Abelian vortices [7, 30, 31].

¹Similar non-Abelian vortices were studied in supersymmetric QCD [12–17] (see refs. [18–21] for a review) and in two-Higgs doublet models (as an extension of the Standard Model) [22–27]. They are different from the system studied here, in the sense that the overall U(1) symmetry is gauged in supersymmetric QCD, and it is an approximate symmetry in two-Higgs doublet models.

A non-Abelian vortex confines bosonic and fermionic gapless modes in its core; the former are Nambu-Goldstone $\mathbb{C}P^2 (\simeq \text{SU}(3)/[\text{SU}(2) \times \text{U}(1)])$ modes originated from spontaneous breaking of the CFL symmetry in the vicinity of the core [7, 10, 5, 11] while the latter are three Majorana fermions [32–34]. Under a rapid rotation, there appear a huge number of vortices (about 10^{19} for typical neutron stars) aligned along the rotation axis, forming a vortex lattice with the lattice spacing of the order of a micrometer [35, 36]. Such vortices penetrate via crossover between the CFL phase and hyperon nuclear matter within a quark-hadron continuity [30, 37–43] without [37] or with Boojums [30, 38, 39]. This direction has stimulated further studies of the Higgs-confinement continuity in the presence of a vortex [43–46].

The CFL phase is characterized by the two diquark condensates of left and right-handed quarks $q_{L,R}$, $(\Phi_{L,R})_{\alpha a} \sim \epsilon_{\alpha\beta\gamma}\epsilon_{abc}q_{L,R}^{\beta b}q_{L,R}^{\gamma c}$ with the color indices $\alpha, \beta, \gamma = r, g, b$ and the flavor indices $a, b, c = u, d, s$. In the ground state, they simultaneously develop vacuum expectation values (VEVs) as $\Phi_L = -\Phi_R$. In the previous studies [6, 9, 5], non-Abelian vortices were constructed in a simplified setup with the assumption $\Phi_L = -\Phi_R$ in the entire region, including vortex cores and the axisymmetry around the vortices. In order to investigate more general vortex configurations, it is convenient to recall a simpler setup of condensed matter systems with simultaneous condensation of two components Φ_1 and Φ_2 . Examples contain two-gap superconductors [47–50], chiral P -wave superconductors [51, 52] and two-component Bose-Einstein condensates (BECs) [53–59], in which the overall phase is a gauge (global) symmetry in the superconductors (BECs), and the relative phase is an approximate global symmetry explicitly broken by a Josephson term (Rabi coupling) $\Phi_1^*\Phi_2 + \text{c.c.}$ (or $\Phi_1^*2\Phi_2^2 + \text{c.c.}$ for chiral P -wave superconductors [51, 52]). A singly-quantized vortex has winding in both components: $\Phi_1 = \Phi_2 \sim e^{i\theta}$ at the same position with the azimuthal angle θ . Depending on the situation, it can be split into two half-quantized vortices $(\Phi_1, \Phi_2) \sim (e^{i\theta}, 1)$ and $(\Phi_1, \Phi_2) \sim (1, e^{i\theta})$ at different positions connected by a sine-Gordon soliton [48–50, 53] (or two domain walls for chiral P -wave superconductors [52]) forming a vortex molecule.²

In this paper, we explore non-Abelian vortex solutions without imposing an Ansatz; no assumption of $\Phi_L = -\Phi_R$ nor of axisymmetry, unlike the previous studies [6, 9, 5]. We find that for certain parameter choices, a single non-Abelian vortex is split into two vortex cores breaking the axisymmetry, each of which has a winding only in left Φ_L or in the right Φ_R condensates. Such constituents are called chiral non-Abelian vortices because a condensate of only left or right chirality has a vortex-winding [63]. Each chiral non-Abelian vortex is attached by one or two domain walls [5, 64], due to the fact that axial and chiral symmetries are explicitly broken by the mass and axial-anomaly terms. The two chiral non-Abelian vortices with opposite chiralities are connected by one or two domain walls forming a non-Abelian vortex molecule. In certain parameter regions, the energy remains axisymmetric, but the vortex centers are not coincident – the axial symmetry is hence broken. We also find, in another parameter region, that the two chiral non-Abelian vortices are confined on a single domain wall, with one domain wall connecting them and

²See ref. [60] for the case of more general higher-order Josephson-like terms and refs. [61, 62] for the cases of more components and corresponding vortex-molecule structures.

two domain walls elongated to spatial infinities.

This paper is organized as follows. In sec. 2 we summarize the Ginzburg-Landau (GL) energy functional of the CFL phase of dense QCD and the ground states of the CFL phase. In sec. 3 we investigate vortex solutions without imposing an Ansatz, and find a non-Abelian vortex molecule in which two chiral vortices of opposite chiralities are connected by one or two domain walls, as well as a vortex molecule confined inside a single domain wall. Sec. 4 is devoted to a summary and discussion.

2 Color-flavor-locked phase of 3-flavor dense QCD

In this section, we review the GL model for the CFL phase to fix our notations, and summarize the ground state structures.

2.1 Ginzburg-Landau model for the color-flavor locked phase

Let $q_{L,R}$ are left- and right-handed quarks. Then, the CFL phase is characterized by the simultaneous diquark condensates of the left and right chiralities:

$$(\Phi_{L,R})_{\alpha a} \sim \epsilon_{\alpha\beta\gamma}\epsilon_{abc}q_{L,R}^{\beta b}q_{L,R}^{\gamma c}, \quad (2.1)$$

which are 3-by-3 matrices of scalar fields with $\alpha, \beta, \gamma = r, g, b = 1, 2, 3$ being color indices and $a, b, c = u, d, s = 1, 2, 3$ being flavor indices. The $SU(3)_C$ color symmetry and $U(1)_B$ baryon symmetry are exact while the $SU(3)_L \times SU(3)_R$ chiral symmetry and $U(1)_A$ axial symmetry are approximate. These symmetries act on the condensates as

$$\begin{aligned} \Phi_L &\rightarrow e^{i\theta_B+i\theta_A}g_C\Phi_L U_L^\dagger, & \Phi_R &\rightarrow e^{i\theta_B-i\theta_A}g_C\Phi_R U_R^\dagger \\ g_C &\in SU(3)_C, & U_{L,R} &\in SU(3)_{L,R}, & e^{i\theta_B} &\in U(1)_B, & e^{i\theta_A} &\in U(1)_A. \end{aligned} \quad (2.2)$$

The vector symmetry $SU(3)_{L+R}$ defined by the condition $U_L = U_R$ is a subgroup of the chiral symmetry $SU(3)_L \times SU(3)_R$, and the rest of generators parametrize Nambu-Goldstone bosons for the chiral symmetry breaking as the coset space $[SU(3)_L \times SU(3)_R]/SU(3)_{L+R} \simeq SU(3)$.

The static Hamiltonian (energy functional) of the GL model takes the form³

$$E = \frac{1}{2g^2}\|F\|^2 + \|d_A\Phi_L\|^2 + \|d_A\Phi_R\|^2 + V, \quad (2.3)$$

$$\begin{aligned} V = &-\frac{m^2}{2}(\|\Phi_L\|^2 + \|\Phi_R\|^2) + \frac{\lambda_1}{4}(\|\Phi_L^\dagger\Phi_L\|^2 + \|\Phi_R^\dagger\Phi_R\|^2) + \frac{\lambda_2}{12}(\|\Phi_L, \Phi_L\|^2 + \|\Phi_R, \Phi_R\|^2) \\ &+ \frac{\lambda_3}{6}\|\Phi_L, \Phi_R\|^2 + \frac{\lambda_4}{2}\|\Phi_L^\dagger\Phi_R\|^2 + \gamma_1(\langle\Phi_L, \Phi_R\rangle + \langle\Phi_L^\dagger, \Phi_R^\dagger\rangle) \\ &+ \gamma_2(\langle\Phi_R^\dagger\Phi_L, \Phi_L^\dagger\Phi_R\rangle + \langle\Phi_L^\dagger\Phi_R, \Phi_R^\dagger\Phi_L\rangle) + \gamma_3 \int_M \star \left(\det(\Phi_L^\dagger\Phi_R) + \det(\Phi_R^\dagger\Phi_L) \right), \end{aligned} \quad (2.4)$$

³The λ_2 and λ_3 terms are divided by $N = 3$ for convenience, compared e.g. with ref. [63].

where the inner product on $M = \mathbb{R}^2$ (the plane orthogonal to vortices) is defined as

$$\langle X, Y \rangle := \text{Tr} \int_M X^\dagger \wedge \star Y, \quad (2.5)$$

where X, Y are both r -forms as well as 3-by-3 complex matrices and \star is the Hodge star mapping r -forms to $(2 - r)$ -forms with the property $\star\star = (-1)^r$ (in two dimensions). The norm squared is then defined as

$$\|X\|^2 := \langle X, X \rangle, \quad (2.6)$$

and finally the double-trace norm squared

$$\|X, Y\|^2 = \int_M \text{Tr}(X^\dagger \wedge \star X) \wedge \star \text{Tr}(Y^\dagger \wedge \star Y). \quad (2.7)$$

The field-strength 2-form for the $\text{SU}(3)_C$ color gauge field is defined as

$$F = dA - A \wedge A = \frac{1}{2} F_{ij} dx^{ij}, \quad (2.8)$$

with the short-hand notation $dx^{ij} := dx^i \wedge dx^j$, $i, j = 1, 2$ and the gauge covariant derivative

$$d_A \phi_{L,R} := d\phi_{L,R} - A\phi_{L,R}, \quad (2.9)$$

where $A = A_i dx^i$ is an anti-Hermitian 1-form, i.e. $A^\dagger = -A$ and is $\mathfrak{su}(3)$ -valued. This implies that it is also traceless.

For convenience, we provide a few expressions in component form

$$\frac{1}{2g^2} \|F\|^2 = -\frac{1}{4g^2} \int_M F_{ij} F^{ij} d^2x \geq 0, \quad (2.10)$$

$$\|d_A \Phi_L\|^2 = \int_M (\partial_i \Phi_L - A_i \Phi_L)^\dagger (\partial^i \Phi_L - A^i \Phi_L) d^2x, \quad (2.11)$$

$$\|\Phi_L\|^2 = \int_M \Phi_L^\dagger \Phi_L d^2x, \quad (2.12)$$

$$\|\Phi_L, \Phi_R\|^2 = \int_M \Phi_L^\dagger \Phi_L \Phi_R^\dagger \Phi_R d^2x, \quad (2.13)$$

$$\langle \Phi_L, \Phi_R \rangle = \int_M \Phi_L^\dagger \Phi_R d^2x, \quad (2.14)$$

where spatial indices i, j are lowered (raised) by the (inverse) metric $g_{ij} = \delta_{ij}$ ($g^{ij} = \delta^{ij}$). Note the negative sign in front of $F_{ij} F^{ij}$ is due to the anti-Hermitian gauge field, i.e. $F^\dagger = -F$.

The GL parameters in the GL model in eq. (2.10) were microscopically calculated in the asymptotically high-density region of QCD [65–67]. In this paper, we leave those parameters as free GL parameters.

2.2 First variation

In order to obtain the equations of motion, we perform a first variation of the energy functional. Let $(A_\tau, \Phi_{L,\tau}, \Phi_{R,\tau})$ be smooth variations of the fields (A, Φ_L, Φ_R) for all τ . Denote by $\alpha = \partial_\tau A_\tau|_{\tau=0}$, $\beta_L = \partial_\tau \Phi_{L,\tau}|_{\tau=0}$ and $\beta_R = \partial_\tau \Phi_{R,\tau}|_{\tau=0}$. We thus obtain

$$\begin{aligned} \frac{d}{d\tau} \Big|_{\tau=0} E &= \langle \beta_L, \text{eom}_{\Phi_L} \rangle_{L^2(M)} + \langle \text{eom}_{\Phi_L}, \beta_L \rangle_{L^2(M)} + \langle \beta_R, \text{eom}_{\Phi_R} \rangle_{L^2(M)} + \langle \text{eom}_{\Phi_R}, \beta_R \rangle_{L^2(M)} \\ &+ \langle \alpha, \text{eom}_A \rangle_{L^2(M)} - \frac{1}{g^2} \text{Tr} \int_M d(\alpha \wedge \star F) \\ &+ \text{Tr} \int_M d \left(\beta_L^\dagger \star d_A \Phi_L + \star d_A \Phi_L^\dagger \beta_L + \beta_R^\dagger \star d_A \Phi_R + \star d_A \Phi_R^\dagger \beta_R \right), \end{aligned} \quad (2.15)$$

with the equations of motion

$$\begin{aligned} \text{eom}_{\Phi_L} &= \delta_A d_A \Phi_L - \frac{m^2}{2} \Phi_L + \frac{\lambda_1}{2} \Phi_L \Phi_L^\dagger \Phi_L + \frac{\lambda_2}{6} \Phi_L \text{Tr}(\Phi_L^\dagger \Phi_L) + \frac{\lambda_3}{6} \Phi_L \text{Tr}(\Phi_R^\dagger \Phi_R) \\ &+ \frac{\lambda_4}{2} \Phi_R \Phi_R^\dagger \Phi_L + \gamma_1 \Phi_R + 2\gamma_2 \Phi_R \Phi_L^\dagger \Phi_R + \gamma_3 \Xi_L, \end{aligned} \quad (2.16)$$

$$\begin{aligned} \text{eom}_{\Phi_R} &= \delta_A d_A \Phi_R - \frac{m^2}{2} \Phi_R + \frac{\lambda_1}{2} \Phi_R \Phi_R^\dagger \Phi_R + \frac{\lambda_2}{6} \Phi_R \text{Tr}(\Phi_R^\dagger \Phi_R) + \frac{\lambda_3}{6} \Phi_R \text{Tr}(\Phi_L^\dagger \Phi_L) \\ &+ \frac{\lambda_4}{2} \Phi_L \Phi_L^\dagger \Phi_R + \gamma_1 \Phi_L + 2\gamma_2 \Phi_L \Phi_R^\dagger \Phi_L + \gamma_3 \Xi_R, \end{aligned} \quad (2.17)$$

$$\begin{aligned} \text{eom}_A &= \frac{1}{g^2} [\delta F + \star A \wedge \star F - \star(\star F \wedge A)] - d_A \Phi_L \Phi_L^\dagger + \Phi_L d_A \Phi_L^\dagger - d_A \Phi_R \Phi_R^\dagger + \Phi_R d_A \Phi_R^\dagger \\ &= \left(-\frac{1}{g^2} \partial^i F_{ij} + \frac{1}{g^2} [A^i, F_{ij}] - (\partial_j \Phi_L - A_j \Phi_L) \Phi_L^\dagger + \Phi_L (\partial_j \Phi_L^\dagger + \Phi_L^\dagger A_j) \right. \\ &\quad \left. - (\partial_j \Phi_R - A_j \Phi_R) \Phi_R^\dagger + \Phi_R (\partial_j \Phi_R^\dagger + \Phi_R^\dagger A_j) \right) dx^j, \end{aligned} \quad (2.18)$$

which are two 0-forms and a 1-form that vanish when the equations of motion are satisfied. In eq. (2.15), the last two terms, being total derivatives, vanish by the assumption of the smooth variations α and β having compact support.⁴ δ_A is the coderivative and δ_A is the gauge covariant coderivative; writing out the $\delta_A d_A$ we obtain

$$\delta_A d_A \Phi_L = -\star d_A \star d_A \Phi_L = -(\partial_i - A_i)(\partial^i - A^i) \Phi_L. \quad (2.19)$$

Finally, the matrices $\Xi_{L,R}$ which are the variation of the determinant, can be written as

$$(\Xi_L)_{\alpha\alpha} = \frac{1}{2} \epsilon_{abc} \epsilon_{def} (\Phi_R)_{\alpha d} (\Phi_L^\dagger \Phi_R)_{be} (\Phi_L^\dagger \Phi_R)_{cf}, \quad (2.20)$$

$$(\Xi_R)_{\alpha\alpha} = \frac{1}{2} \epsilon_{abc} \epsilon_{def} (\Phi_L)_{\alpha d} (\Phi_R^\dagger \Phi_L)_{be} (\Phi_R^\dagger \Phi_L)_{cf}. \quad (2.21)$$

Having the equations of motion in hand, we can read off the perturbative masses from the linearized equations:

$$m_\Phi = \frac{m}{\sqrt{2}}, \quad m_A = g \sqrt{2(v_L^2 + v_R^2)}, \quad (2.22)$$

with the two VEVs $v_L = \langle \Phi_L \rangle$ and $v_R = \langle \Phi_R \rangle$ being determined by the ground state equations, see below.

⁴From a physical point of view, the finite-energy condition requires F and $d_A \Phi_{L,R}$ to vanish a spatial infinity and hence the total derivatives vanish.

2.3 Ground states

Let us assume that the ground states are given by diagonal matrices, which thus do not break the $SU(3)_{C+L+R}$ symmetry. We will further use the $U(1)_{A,B}$ symmetries to set the phases of the VEVs to zero (or π) if possible.

Let us consider the ground state with only $m \neq 0$, $\lambda_1 > 0$, $\lambda_2 > 0$. The ground state solution compatible is unique

$$\Phi_L = -\Phi_R = v\mathbf{1}_3, \quad v = \frac{m}{\sqrt{\lambda_1 + \lambda_2}}, \quad \langle V \rangle = -\frac{3m^4}{2(\lambda_1 + \lambda_2)}, \quad (2.23)$$

where $\langle V \rangle$ is the potential value at the VEV. The symmetry is broken to the CFL symmetry $SU(3)_{C+L+R}$ given by $g_C = U_L = U_R$ in eq. (2.2).

Turning on the mixed Hermitian terms, $\lambda_3 > 0$ and $\lambda_4 > 0$, two competing ground states appear:

$$\Phi_L = -\Phi_R = u\mathbf{1}_3, \quad u = \frac{m}{\sqrt{\lambda_1 + \lambda_2 + \lambda_3 + \lambda_4}}, \quad \langle V \rangle = -\frac{3m^4}{2(\lambda_1 + \lambda_2 + \lambda_3 + \lambda_4)}, \quad (2.24)$$

and

$$\left\{ \begin{array}{l} \Phi_L = v\mathbf{1}_3 \\ \Phi_R = \mathbf{0}_3 \end{array} \right\} \quad \text{or} \quad \left\{ \begin{array}{l} \Phi_L = \mathbf{0}_3 \\ \Phi_R = v\mathbf{1}_3 \end{array} \right\}, \quad v = \frac{m}{\sqrt{\lambda_1 + \lambda_2}}, \quad \langle V \rangle = -\frac{3m^4}{4(\lambda_1 + \lambda_2)}. \quad (2.25)$$

The condition for the ground state being either the v or the u ground state is

$$\lambda_1 + \lambda_2 > \lambda_3 + \lambda_4 : \quad \Rightarrow \quad \Phi_L = -\Phi_R = u\mathbf{1}_3, \quad (2.26)$$

$$\lambda_1 + \lambda_2 < \lambda_3 + \lambda_4 : \quad \Rightarrow \quad \left\{ \begin{array}{l} \Phi_L = v\mathbf{1}_3 \\ \Phi_R = \mathbf{0}_3 \end{array} \right\} \quad \text{or} \quad \left\{ \begin{array}{l} \Phi_L = \mathbf{0}_3 \\ \Phi_R = v\mathbf{1}_3 \end{array} \right\}. \quad (2.27)$$

The former is still the conventional CFL ground state with the CFL symmetry, while the latter ground state of the v -ground state (requiring large λ_3 or λ_4) contains two degenerate ground states and hence a domain wall that connects them.

We will now turn on $\gamma_1 \neq 0$. There will still be two competing ground states that depend on the whether λ_3 or λ_4 (or both) is large or not. Due to the linear term (proportional to γ_1) in the ground state equations, the vanishing VEV from before is shifted slightly. For convenience we include γ_2 although it is allowed to vanish in the following ground state. In particular, we get

$$\Phi_L = -\text{sign}(\gamma_1)\Phi_R = w\mathbf{1}_3, \quad w = \sqrt{\frac{m^2 + 2|\gamma_1|}{\lambda_1 + \lambda_2 + \lambda_3 + \lambda_4 + 4\gamma_2}},$$

$$\langle V \rangle = -\frac{3(m^2 + 2|\gamma_1|)^2}{2(\lambda_1 + \lambda_2 + \lambda_3 + \lambda_4 + 4\gamma_2)}, \quad (2.28)$$

when the condition

$$2 \left(1 + \frac{2|\gamma_1|}{m^2} \right)^2 > \left(1 + \frac{\lambda_3 + \lambda_4}{\lambda_1 + \lambda_2} \right) \left(1 + \frac{2\gamma_1^2(\lambda_1 + \lambda_2)}{m^4(\lambda_3 + \lambda_4 - \lambda_1 - \lambda_2 + 4\gamma_2)} \right), \quad (2.29)$$

is satisfied and otherwise the following is the ground state

$$\begin{aligned}
\Phi_L &= w_{\pm}, & \Phi_R &= -\text{sign}(\gamma_1)w_{\mp}, \\
w_{\pm} &= \frac{m}{\sqrt{\lambda_1 + \lambda_2}} \sqrt{\frac{1}{2} \pm \epsilon \sqrt{1 - \frac{16\gamma_1^2(\lambda_1 + \lambda_2)^2}{m^4(\lambda_3 + \lambda_4 - \lambda_1 - \lambda_2 + 4\gamma_2)^2}}}, \\
\langle V \rangle &= -\frac{3m^4}{4(\lambda_1 + \lambda_2)} - \frac{6\gamma_1^2}{\lambda_3 + \lambda_4 - \lambda_1 - \lambda_2 + 4\gamma_2},
\end{aligned} \tag{2.30}$$

with the sign $\epsilon = \text{sign}[\lambda_3 + \lambda_4 - \lambda_1 - \lambda_2 + 4\gamma_2]$. The condition (2.29) choosing between the two types of ground states clearly gets complicated by the presence of γ_1 – the Josephson term, but the ground state structure is changed only little by γ_2 . Interestingly, γ_2 does not affect the ground state condition when $\gamma_1 = 0$. One can check that setting $\gamma_1 := 0$, the condition (2.29) reduces to the previous condition, i.e. $\lambda_1 + \lambda_2 > \lambda_3 + \lambda_4$.

Clearly the ground state structure becomes only more complicated by turning on $\gamma_3 \neq 0$. We will focus on the simplest case where we turn on $\gamma_3 \neq 0$ but leave $\gamma_1 = \gamma_2 = 0$. In this case, there is only a single ground state

$$\begin{aligned}
\Phi_L &= -\Phi_R = r\mathbf{1}_3, & r &= \frac{1}{2} \sqrt{\frac{\lambda_{1234} - \sqrt{\lambda_{1234}^2 - 8m^2|\gamma_3|}}{|\gamma_3|}}, \\
\langle V \rangle &= -\frac{(\lambda_{1234} - \sqrt{\lambda_{1234}^2 - 8m^2|\gamma_3|}) (16m^2|\gamma_3| - \lambda_{1234} (\lambda_{1234} - \sqrt{\lambda_{1234}^2 - 8m^2|\gamma_3|}))}{32\gamma_3^2},
\end{aligned} \tag{2.31}$$

provided that γ_3 is small enough:

$$|\gamma_3| < \frac{\lambda_{1234}^2}{8m^2}, \tag{2.32}$$

and we have defined $\lambda_{1234} := \sum_{i=1}^4 \lambda_i$. If on the other hand, the above condition for $|\gamma_3|$ is not satisfied, the ground state becomes that of the partially unbroken phase:

$$\left\{ \begin{array}{l} \Phi_L = v\mathbf{1}_3 \\ \Phi_R = \mathbf{0}_3 \end{array} \right\} \text{ or } \left\{ \begin{array}{l} \Phi_L = \mathbf{0}_3 \\ \Phi_R = v\mathbf{1}_3 \end{array} \right\}, \quad v = \frac{m}{\sqrt{\lambda_1 + \lambda_2}}, \quad \langle V \rangle = -\frac{3m^4}{4(\lambda_1 + \lambda_2)}. \tag{2.33}$$

A comment in store about the γ_3 term, is that the potential theoretically has runaway directions that can be triggered for very large field values. This must however physically be just an artifact of the low-energy EFT.

3 Chiral vortex molecules

In this section, we numerically construct non-axisymmetric vortex configurations such as chiral vortex molecules and chiral vortices confined on a domain wall.

3.1 Vortex Ansätze for initial conditions

We seek solutions that describe vortex molecules that hence do not possess axial symmetry. Nevertheless, the initial configurations for our simulation need an Ansatz for each of the two vortices, which will be detailed here. The chiral $(1, 0)$ vortex is given by

$$\Phi_L = v_L \text{diag} \left(f(r) e^{i\theta}, 1, 1 \right), \quad \Phi_R = v_R \text{diag}(1, 1, 1), \quad A = -i\epsilon_{ij} \frac{x^j}{2r^2} a(r) T dx^i, \quad (3.1)$$

with the matrix $T = \text{diag}(\frac{2}{3}, -\frac{1}{3}, -\frac{1}{3})$ and the VEV of Φ_L (Φ_R) being v_L (v_R), depending on the ground state in question. Similarly, the chiral $(0, 1)$ vortex is given by

$$\Phi_L = v_L \text{diag}(1, 1, 1), \quad \Phi_R = v_R \text{diag} \left(f(r) e^{i\theta}, 1, 1 \right), \quad A = -i\epsilon_{ij} \frac{x^j}{2r^2} a(r) T dx^i, \quad (3.2)$$

with the matrix $T = \text{diag}(\frac{2}{3}, -\frac{1}{3}, -\frac{1}{3})$ and the VEV of Φ_L (Φ_R) being v_L (v_R), depending on the ground state in question.

In order to understand the normalization of the gauge field, we consider the split of the winding of the scalar field in eq. (3.1) into the global $U(1)_B$, $U(1)_A$, $SU(3)_L$ and $SU(3)_R$ with right action as well as the local $SU(3)_C$ with a left action:

$$\text{diag} \left(f(r) e^{i\theta}, 1, 1 \right) = e^{i\beta\theta T} \text{diag} (f(r), 1, 1) e^{i\beta\theta T} e^{i\alpha\theta} e^{i\alpha\theta}, \quad (3.3)$$

$$\text{diag} (1, 1, 1) = e^{i\beta\theta T} \text{diag} (1, 1, 1) e^{-i\beta\theta T} e^{i\alpha\theta} e^{-i\alpha\theta}. \quad (3.4)$$

The second equation, corresponding to the right field is trivially solved by any α and any β , whereas the first equation leads to two equations: $\frac{4}{3}\beta + 2\alpha = 1$ and $-\frac{2}{3}\beta + 2\alpha = 0$, yielding $\alpha = \frac{1}{6}$ and $\beta = \frac{1}{2}$. This means that the gauge part of the vortex carries the flux $\frac{1}{2}T$, which indeed is the normalization of the gauge field in eq. (3.1).

The boundary conditions for the two profile functions are

$$f(0) = 0, \quad a(0) = 0, \quad f(\infty) = 1, \quad a(\infty) = 1. \quad (3.5)$$

A suitable initial guess for the profile functions takes the perturbative masses into account

$$f_{\text{guess}}(r) = \tanh(m_\Phi r), \quad a_{\text{guess}}(r) = \tanh(m_A r). \quad (3.6)$$

For the initial state, we prepare a $(1, 0)$ and a $(0, 1)$ vortex with large enough separation that we can assume the following Abrikosov Ansatz

$$\begin{aligned} \Phi_L &= v_L \text{diag} \left(f(r_L) e^{i\theta_L}, 1, 1 \right), & \Phi_R &= v_R \text{diag} \left(f(r_R) e^{i\theta_R}, 1, 1 \right), \\ A &= -\epsilon_{ij} \left(\frac{x_L^j}{2r_L^2} a(r_L) + \frac{x_R^j}{2r_R^2} a(r_R) \right) T dx^i, \end{aligned} \quad (3.7)$$

with $x + L + iy = r_L e^{i\theta_L}$ and $x - L + iy = r_R e^{i\theta_R}$ being two radial coordinates centered at the left and the right-hand side vortex, respectively.

The terms with the coefficients $\gamma_{1,2,3}$ give direct couplings between the left Φ_L and right Φ_R condensates. When all $\gamma_{1,2,3}$ are turned off, chiral vortices $(1, 0)$ and $(0, 1)$ are

deconfined; they are attached by no domain walls. If we turn on at least one of $\gamma_{1,2,3}$, they are attached by one or two domain walls [63], as axion strings. This can be confirmed by substituting the Ansätze in eq. (3.1) or (3.2) into the potential term and by evaluating it at a large circle encircling a vortex. We then obtain a sine-Gordon model (when only one of $\gamma_{1,2,3} \neq 0$), a double sine-Gordon model (when $\gamma_{1,2} \neq 0$ and $\gamma_3 = 0$) and so on. The effective sine-Gordon models count the number of domain walls attached to the vortex that we are considering.⁵ In particular, in the case of $\gamma_{1,2} \neq 0$ and $\gamma_3 = 0$, the domain walls are non-Abelian sine-Gordon solitons carrying $\mathbb{C}P^2$ moduli [68, 69].⁶ When a chiral vortex is attached to a non-Abelian sine-Gordon soliton their $\mathbb{C}P^2$ moduli match. The term with $\gamma_3 \neq 0$ somehow “Abelianizes” the $\mathbb{C}P^2$ moduli.

3.2 Diagonal matrices

In ref. [63] it was shown that $\mathbb{C}P^2$ moduli attract energetically. Under this assumption, choosing one vortex, say the left vortex in Φ_L to be on diagonal form (without loss of generality), the right vortex in Φ_R will align with the other and hence also be on diagonal form. Although we do not limit our simulations to diagonal matrices, a faster version that operates only using diagonal matrices can speed up the numerical investigations. For this reason we give the following Lemma.

Lemma 1 *The variational equations (2.16)-(2.18) remain diagonal matrices when sourced by initial conditions that consist of diagonal matrices.*

Proof: In order to facilitate the proof, we assume that the numerical method updates the fields by adding a constant times the eom for that field to itself at every step. This is the case for the method given in sec. 3.3. It remains to check that the eom of eqs. (2.16)-(2.18) are diagonal matrices if the Φ_L , Φ_R , A all are. Since the trace preserves the diagonal structure and the variational equations consist of products of diagonal matrices, only the symbols $\Xi_{L,R}$ need to be checked. An explicit calculation reveals that $\Phi_{L,R}$ being diagonal matrices reduces the variation of the determinant to

$$(\Xi_L)_{\alpha\alpha} = \frac{1}{2} \sum_{b,c=1}^3 \epsilon_{abc} \epsilon_{abc} (\Phi_R)_{\alpha\alpha} (\Phi_L^\dagger \Phi_R)_{bb} (\Phi_L^\dagger \Phi_R)_{cc}, \quad (3.8)$$

which vanishes when $\alpha \neq a$ and similarly for Ξ_R . □

3.3 Numerical method

We will utilize the numerical method sometimes called arrested Newton flow, which similarly to relativistic dynamics accelerates towards the nearest local minimum of the energy

⁵In the two-Higgs doublet models as an extension of the Standard Model, a single non-Abelian vortex is attached by one or two domain walls depending on the parameters as shown by the same analysis [22, 23]. This model also admits a molecule of two non-Abelian vortex strings [27].

⁶The $U(N)$ non-Abelian sine-Gordon model appears also in the $U(N)$ chiral Lagrangian [70] and on a Josephson junction of two color superconductors [71–73], and a sine-Gordon soliton can host $SU(N)$ Skyrmions as $\mathbb{C}P^{N-1}$ lumps [69, 74, 73].

functional. Unlike relativistic dynamics, the arrested part of the method is a continuous monitoring of the static energy (potential energy including field gradients) which sets the kinetic energy of the flow to zero once the energy increases. Specifically, we solve the equations

$$\partial_\tau^2 \Phi_L = -\text{eom}_{\Phi_L}, \quad \partial_\tau^2 \Phi_R = -\text{eom}_{\Phi_R}, \quad \partial_\tau^2 A = -\text{eom}_A, \quad (3.9)$$

with an initial condition given in sec. 3.1 with L typically set to $L := 4$. τ is not real time, but simply a parametrization of the flow. At every step of the flow, we compute the energy E of eq. (2.3) and compare it with the energy of the previous step. If the energy has increased, we set $\partial_\tau \Phi_L = \partial_\tau \Phi_R = \partial_\tau A = 0$.

The numerical computations are performed on square lattices with 1024^2 lattice sites and the discrete derivatives are approximated using a 5-point stencil and a 4th-order numerical derivative. The lattice spacing is typically 0.0391.

3.4 Numerical results

We will now perform numerical computations with the method described in sec. 3.3 and the initial conditions given in sec. 3.1. The main results are for the $(1, 0) + (0, 1)$ vortices, each with winding in the 11 components of both the left and right scalar fields. Due to the large parameter space of the model (9-dimensional parameter space) and large number of possible initial conditions (relative $\mathbb{C}P^2$ coordinate), we cannot claim that we have exhausted all possibilities, but we get a general picture of how the set of chiral vortices behave. Also for simplicity, we will henceforth set $g := 1$ and $m := \sqrt{2}$.

Starting with the most simplistic choice of the potential parameters, we turn on only λ_1 (here and henceforth, the parameters λ_1 through λ_4 and γ_1 through γ_3 vanish when not turned on), i.e. we will set $\lambda_1 := 2$. We are surprised to see that the two vortices attract and form a coincident vortex with total winding $(1, 1)$, see fig. 1. The left and right fields' vortices are completely coincident and the energy has eccentricity zero, where we define the eccentricity as⁷

$$e = \sqrt{1 - \frac{\int_M \star(x - x_{\text{CM}})^2 \mathcal{E}}{\int_M \star(y - y_{\text{CM}})^2 \mathcal{E}}}, \quad (3.10)$$

where center of mass is defined as $(x_{\text{CM}}, y_{\text{CM}}) = \int_M \star(x, y) \mathcal{E}$ and the energy density is defined by $E = \int_M \star \mathcal{E}$ and E is the energy given in eq. (2.3). Eccentricity zero corresponds to an axially symmetric energy configuration.

In the figure, we can clearly see the vortex “zero” in the 11 component of both the left and right scalar fields. Due to the gauge field being $\text{SU}(3)$ and hence traceless, the gauge field must turn on the 22 and 33 components, which in turn induce nontrivial behavior in the the 22 and 33 component of both the scalar fields. The “dip” in the 22 and 33 components of the scalar fields is, however, quite mild. The gauge field being $\text{SU}(3)$ also

⁷We assume here that the configuration is elliptic with the major axis along the x -direction; otherwise the inverse of the fraction in the square root need to be used.

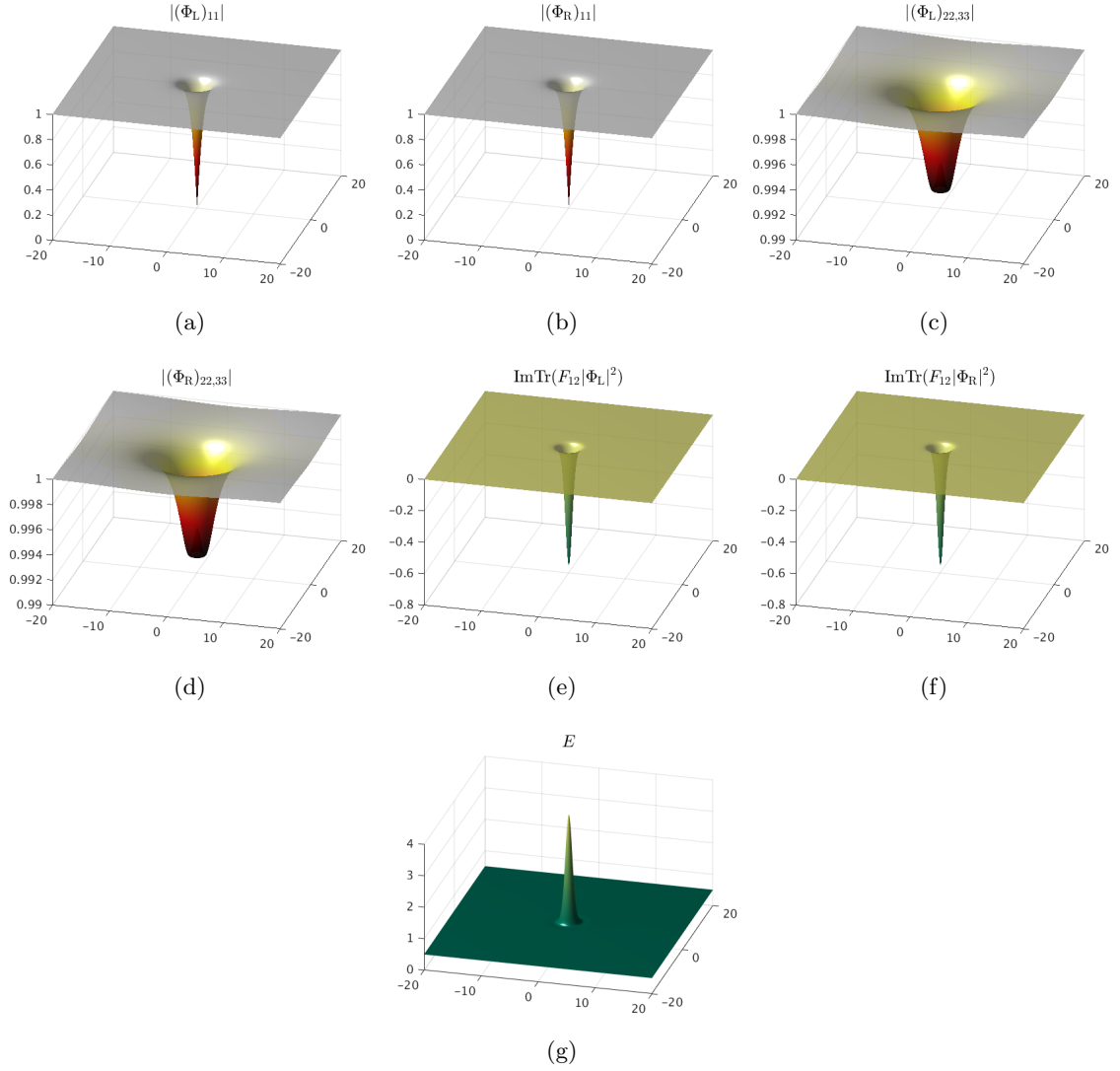


Figure 1. “Regular” (axisymmetric) non-Abelian vortex, i.e. no γ terms turned on. In this figure $g = 1$, $m = \sqrt{2}$, $\lambda_{1,2,3,4} = (2, 0, 0, 0)$, $\gamma_{1,2,3} = (0, 0, 0)$. This vortex configuration has winding number $(1, 1)$, the left and right fields’ vortices are coincident and the energy is axially symmetric ($e = 0$).

implies that its field strength F_{12} is traceless. The non-Abelian part of the field strength is, however, not gauge invariant. We thus display a gauge invariant quantity constructed out of the non-Abelian field strength as well as the two scalar fields

$$\text{Im}[\text{Tr}[F_{12}\Phi_L\Phi_L^\dagger]], \quad \text{Im}[\text{Tr}[F_{12}\Phi_R\Phi_R^\dagger]], \quad (3.11)$$

where taking the imaginary part is simply due to the convention of using anti-Hermitian gauge fields. The reason for multiplying by $\Phi_L\Phi_L^\dagger$ is that it is a matrix in color indices (i.e. with the flavors traced over).

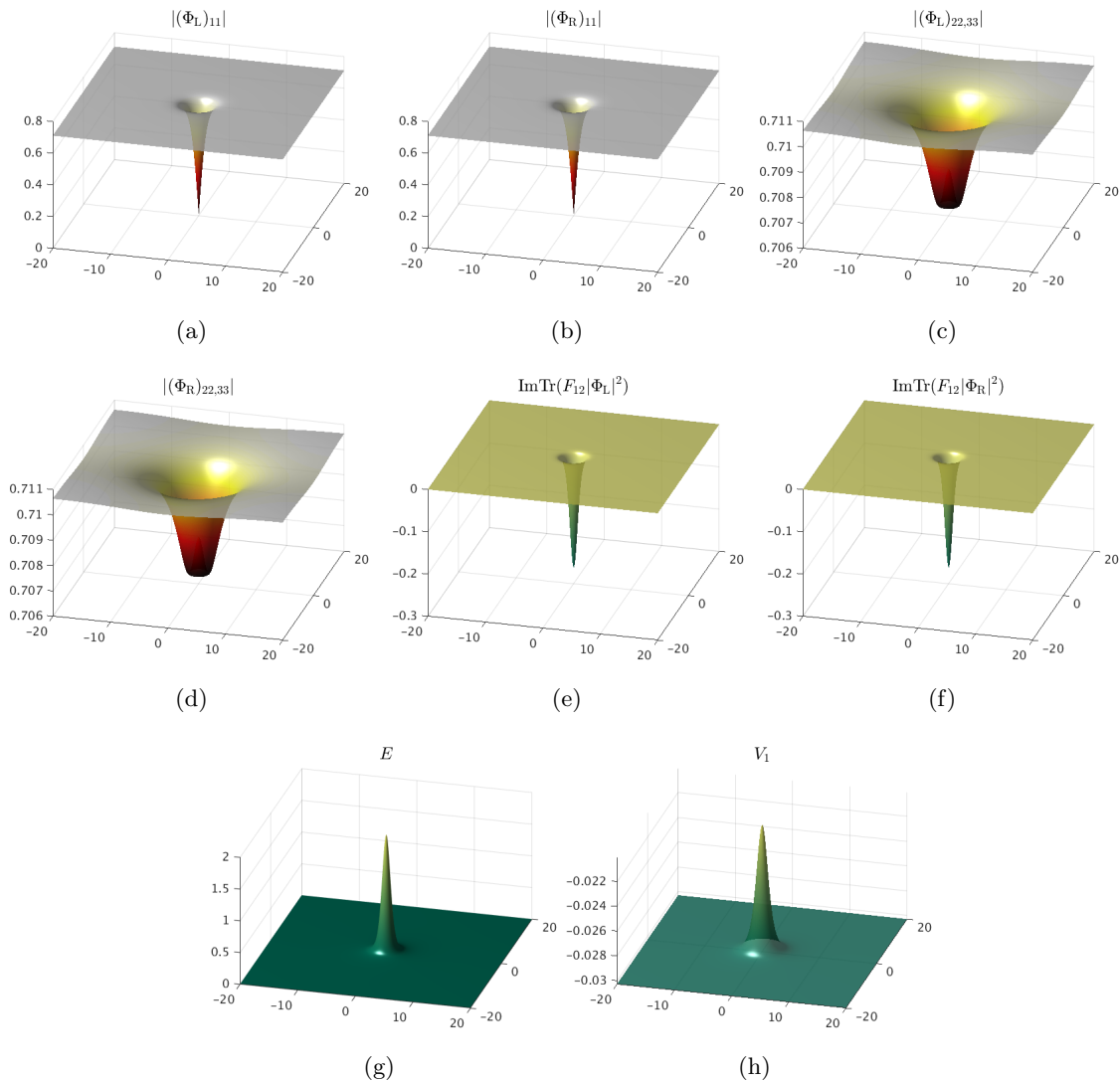


Figure 2. Confined chiral vortices. In this figure $g = 1$, $m = \sqrt{2}$, $\lambda_{1,2,3,4} = (3, 0, 0, 1)$, $\gamma_{1,2,3} = (-0.01, 0, 0)$. This vortex configuration has winding number $(1, 1)$, the left and right fields' vortices are coincident and the energy is axially symmetric ($\mathbf{e} = 0$).

In fig. 2, we turn on the λ_4 and also the Josephson term, i.e. γ_1 . λ_4 does not have much impact on the vortex configuration, as long as it is smaller than λ_1 . Taking it larger

than λ_1 changes the ground state structure, but as we will see shortly, once it is of the same magnitude as λ_1 , it will have an impact on the outcome.

By the logic that the Josephson term (γ_1) attaches one domain wall connecting the left and right chiral vortices, whereas the γ_2 term attaches two domain walls between the pair of vortices [63], we can predict that the tension of the Josephson wall will give rise to further attraction. In the example given in fig. 2, this is indeed the case, but since the vortices already want to be coincident, nothing much can be seen from turning on the Josephson term ($\gamma_1 \neq 0$).

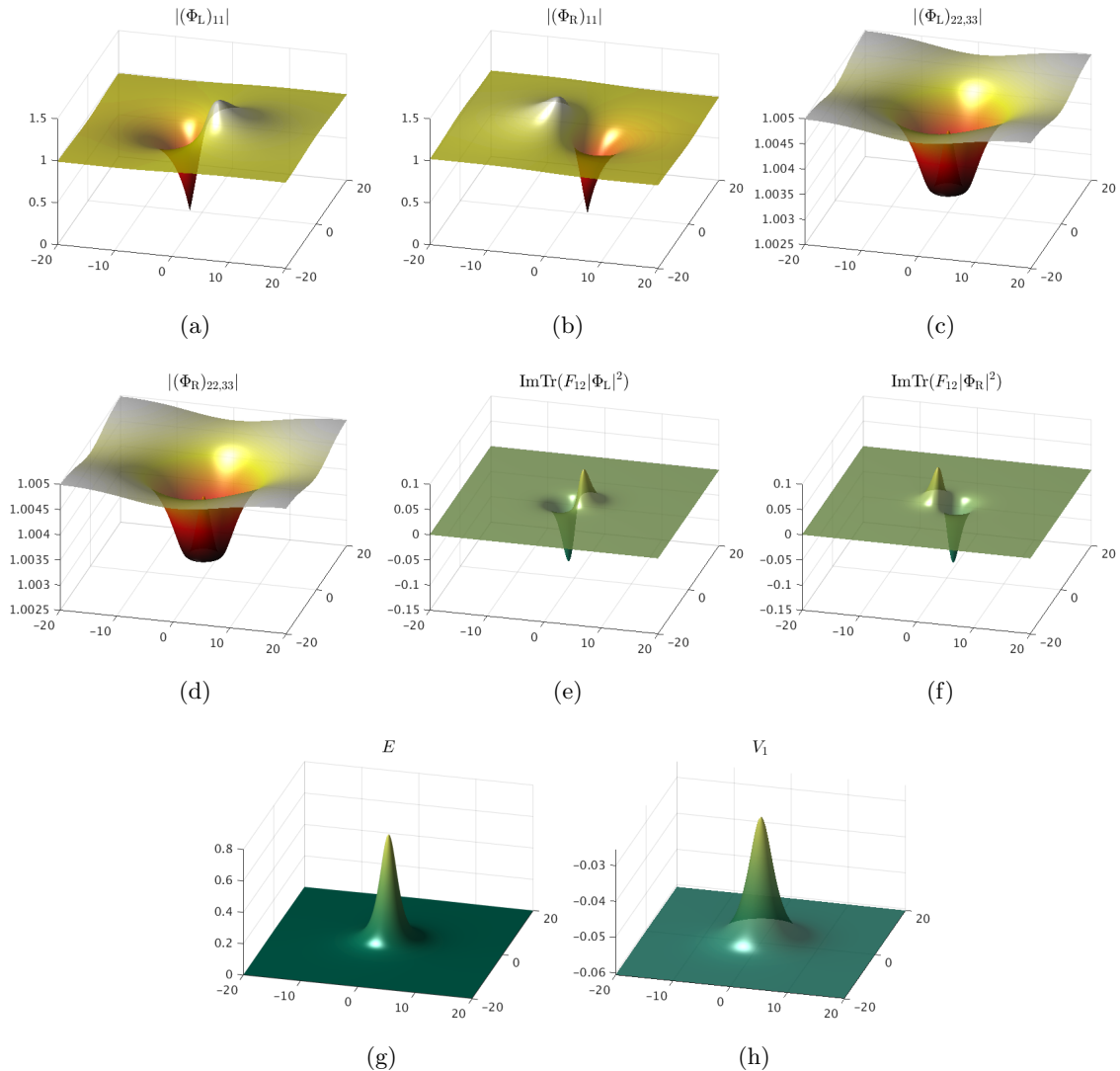


Figure 3. Dipolar chiral vortices. In this figure $g = 1$, $m = \sqrt{2}$, $\lambda_{1,2,3,4} = (1, 0, 0, 1)$, $\gamma_{1,2,3} = (-0.01, 0, 0)$. This vortex configuration has winding number $(1, 1)$, the left and right fields' vortices form a dipole but the energy is axially symmetric ($e = 0$). The scalar fields break the axial symmetry though.

In order to provoke some nontrivial structure out of the composite chiral vortices that like to be sitting in a coincident bound state, we leave the Josephson term on $\gamma_1 \neq 0$, but

lower λ_1 to the same level of λ_4 , see fig. 3. This gives rise to a repulsion of the left and right chiral vortices, that are, however, still confined by the Josephson wall. Interestingly, although the scalar field clearly have distinct zeros (non-coincident) the energy is nevertheless axially symmetric. In that sense, just like a magnet, the bound state is dipolar with the two zeros forming the two poles of the state, which however remains axially symmetric in terms of the energy density. The eccentricity thus remains vanishing. In fig. 3 we also display V_1 which is the γ_1 part of V (see eq. (2.4)).

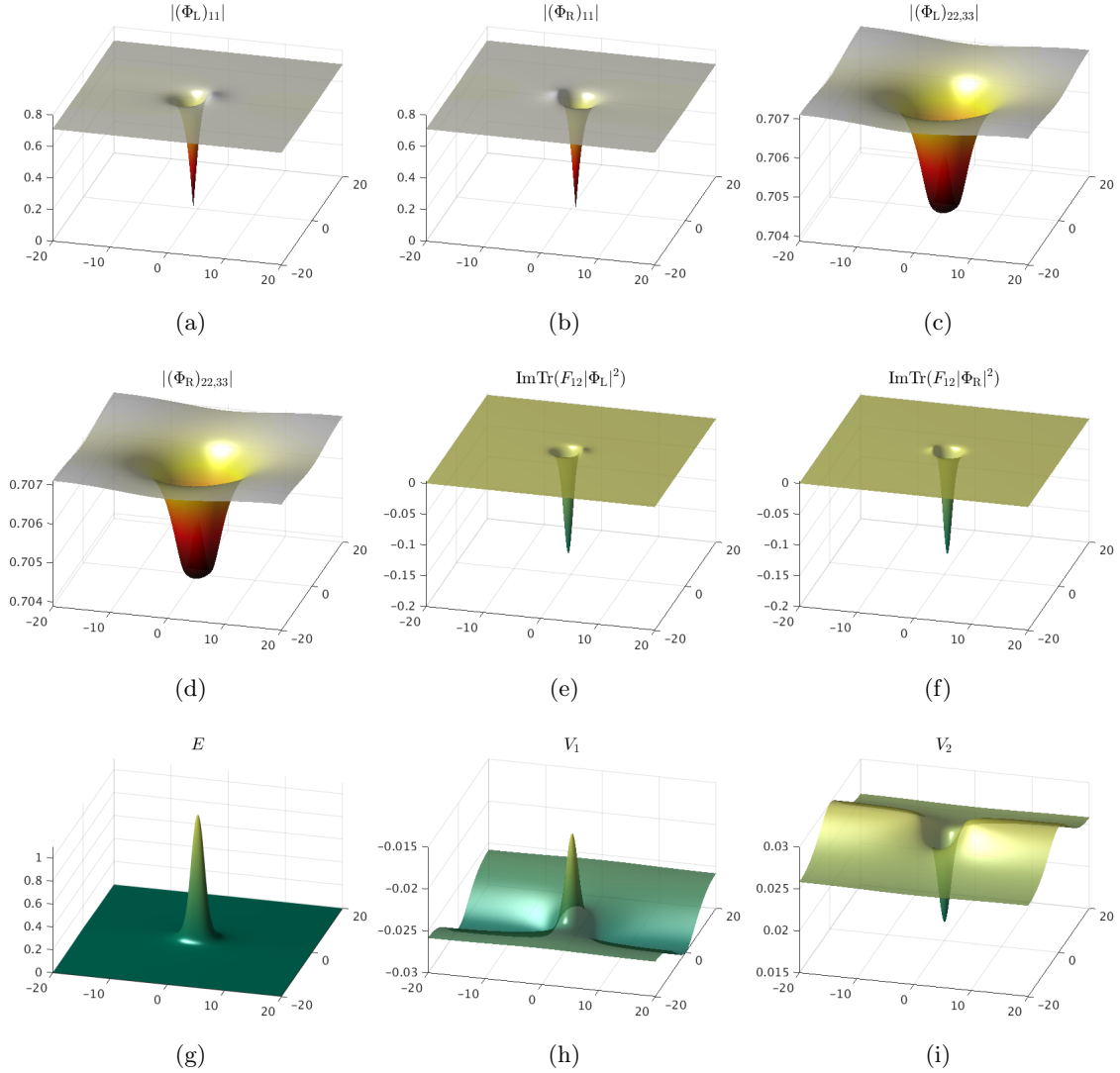


Figure 4. Chiral vortices with both Josephson and Josephson-squared terms turned on. In this figure $g = 1$, $m = \sqrt{2}$, $\lambda_{1,2,3,4} = (3, 0, 0, 1)$, $\gamma_{1,2,3} = (-0.01, 0.01, 0)$. This vortex configuration has winding number $(1, 1)$, the left and right fields' vortices form a dipole and energy density is elliptic with eccentricity $e = 0.71$. The vortex dipolar molecule lives on an infinite Josephson wall, which however has vanishing energy density.

The way the Josephson term (γ_1) and its squared generalization (γ_2) connects to two vortices depends on the sign of the coefficients (or alternatively also on how the winding of

the vortices is chosen; for example with $\gamma_2 = \gamma_3 = 0$ the configurations are symmetric under $\gamma_1 \rightarrow -\gamma_1$ and $\Phi_R \rightarrow -\Phi_R$. In particular, the Josephson walls can form infinite domain walls. In fact, the non-axially symmetric vortex configuration shown in fig. 4 is created by having each vortex (i.e. left and right vortices) have a γ_1 -wall that tends off to infinity, but meticulously choosing the γ_2 term with the exact same magnitude and opposite sign. This creates a small molecular (dipolar) bound state of left and right vortices, that are connected with one γ_1 -wall, but have the other two γ_2 -walls tending off to spatial infinity (recall that the γ_2 term attaches two walls to each vortex). Because of the fine tuned magnitude and opposite sign of the couplings $\gamma_2 = -\gamma_1$, the energy of the wall tending off to infinity cancel out exactly (see V_1 and V_2 in fig. 4), leaving behind a confined albeit non-axially symmetric dipolar molecule of chiral vortices.⁸

Now if we do not fine tune the cancellation between the Josephson term and its squared counterpart, we will create a domain wall with finite energy, see fig. 5. Increasing γ_2 creates an infinite double Josephson wall from each vortex. They are repelled slightly by the γ_1 term and confined by the γ_2 term, which however also gives an infinite contribution to the energy (if space is taken to be \mathbb{R}^2). This chiral vortex configuration is truly a molecule of $(1, 0)$ and $(0, 1)$ vortices with a visible separation (non-coincidence) in both the field zeros and in the energy density.

There are many other configurations that are very similar in nature to the examples we have selected above. As long as the ground state conditions allow for the same fully broken and symmetric (up to a phase or sign) ground state, many sets of coupling values give rise to very similar types of chiral vortex bound states. In fig. 6, we give an example of changing the γ_1 term for the γ_3 term in the configuration shown in fig. 2, yielding a very similar result. Another rule of thumb is that interpolating between λ_1 and λ_2 gives rise to the same type of configurations; the same holds true for interpolating between λ_3 and λ_4 .

One aspect of the huge parameter space that we left out in the above results, is the fact that the left $(1, 0)$ vortex and the right $(0, 1)$ vortex can both be rotated around in $\mathbb{C}P^2$. The overall rotation (i.e. of both vortices) makes no difference in the energy density. However, there is a whole $\mathbb{C}P^2$ space of *relative* orientations, for example fixing the left vortex to be in the 11 component, the right vortex could be rotated to other points of $\mathbb{C}P^2$. We know from ref. [63] that orthogonal vortices have larger energies than parallel. Let us fix the left vortex in the 11 component of Φ_L . The latter statement says that the energy is larger if we place the right vortex in the 22 component of Φ_R than if we place it in the 11 component. One may contemplate what happens in between these two points of $\mathbb{C}P^2$. Using a rotation matrix of the form

$$U(\varphi) = \begin{pmatrix} \cos \varphi & \sin \varphi & 0 \\ -\sin \varphi & \cos \varphi & 0 \\ 0 & 0 & 1 \end{pmatrix}, \quad (3.12)$$

⁸This resembles a domain-wall bimeron in chiral magnets [75].

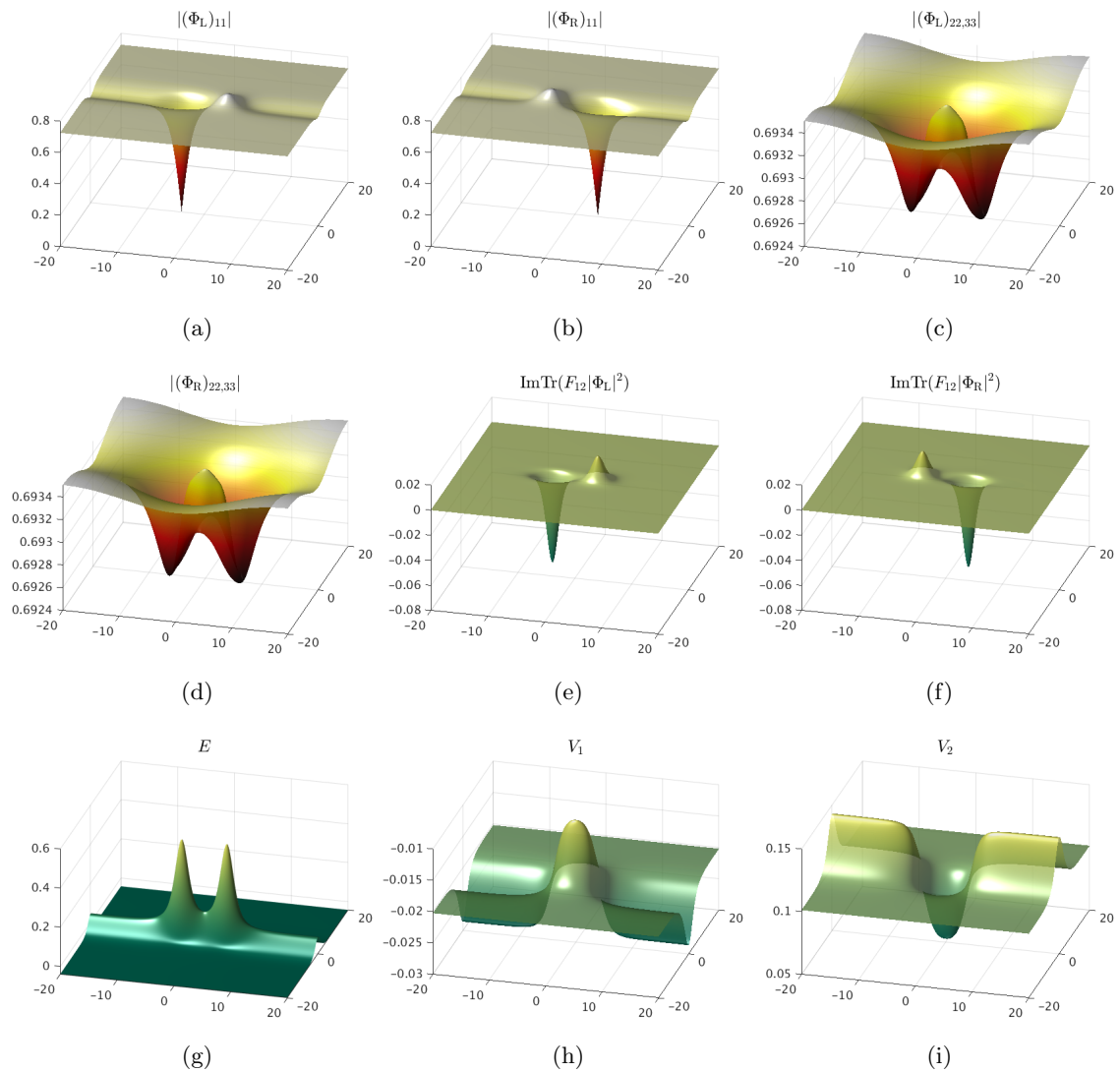


Figure 5. Chiral vortices as beats on a wall (Josephson double domain wall from the Josephson-squared term). In this figure $g = 1$, $m = \sqrt{2}$, $\lambda_{1,2,3,4} = (3, 0, 0, 1)$, $\gamma_{1,2,3} = (-0.01, 0.05, 0)$. This vortex configuration has winding number $(1, 1)$, the left and right fields' vortices form a dipole and energy density is elliptic with eccentricity $e = 0.95$ (computed on the domain of the figure). The vortex dipolar molecule lives on an infinite Josephson wall with finite tension.

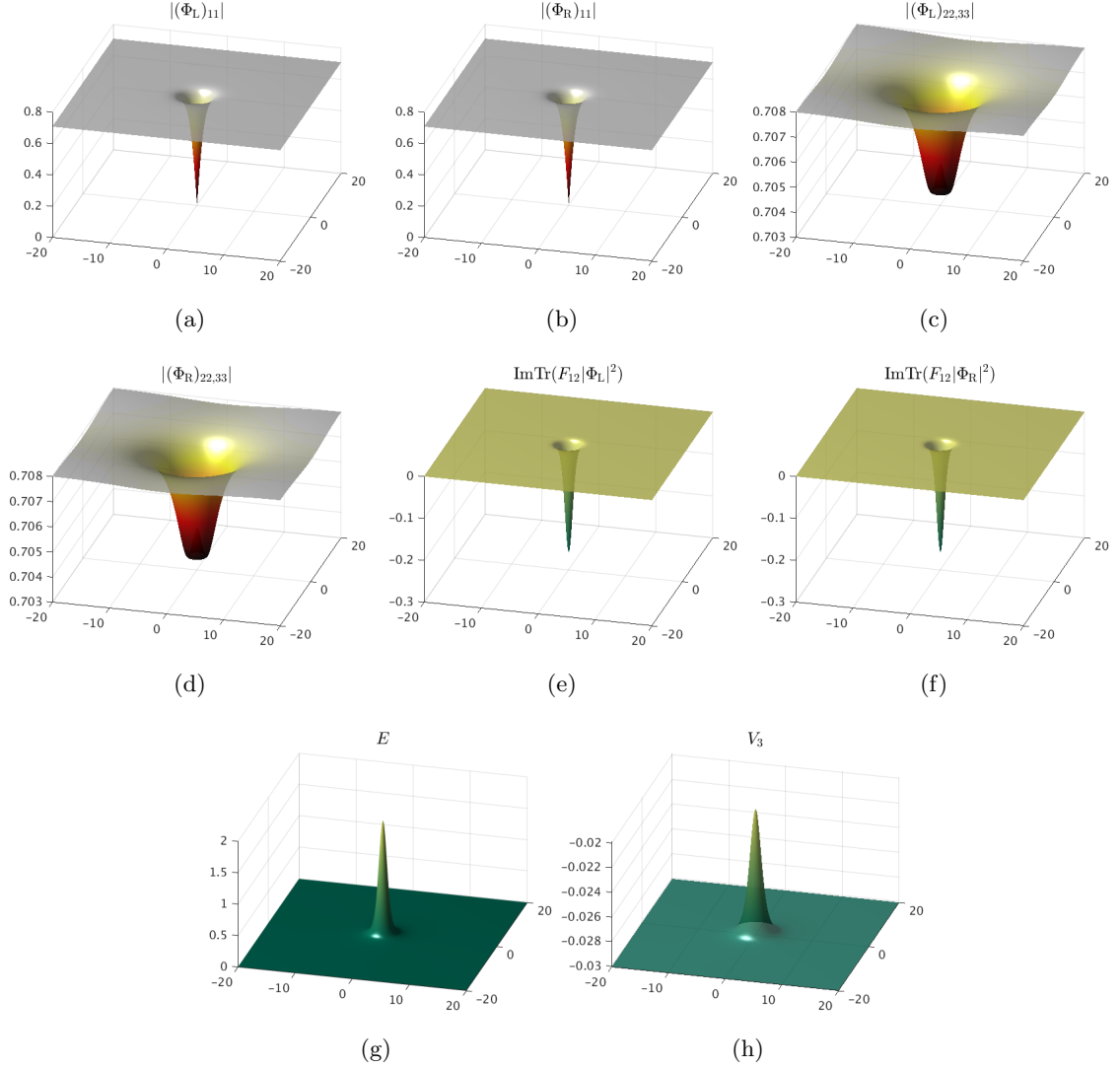


Figure 6. Confined vortices with the γ_3 term. In this figure $g = 1$, $m = \sqrt{2}$, $\lambda_{1,2,3,4} = (3, 0, 0, 1)$, $\gamma_{1,2,3} = (0, 0, -0.01)$. This vortex configuration has winding number $(1, 1)$, the left and right fields' vortices are coincident and the energy is axially symmetric ($e = 0$).

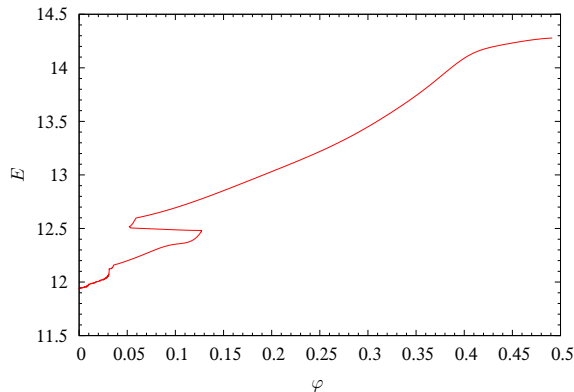


Figure 7. Energy during a flow for a configuration with the left vortex in the 11 component and the right vortex in the 22 component. The flow minimizes the energy, eventually aligning the two vortices in $\mathbb{C}P^2$. For details of the angle φ , see the text.

and rotating the fields as

$$\begin{aligned} \Phi_L &= v_L \text{diag} (f(r_L)e^{i\theta_L}, 1, 1), & \Phi_R &= v_R U \text{diag} (f(r_R)e^{i\theta_R}, 1, 1)U^\dagger, \\ A &= -\epsilon_{ij} \left(\frac{x_L^j}{2r_L^2} a(r_L)T + \frac{x_R^j}{2r_R^2} a(r_R)UTU^\dagger \right) dx^i, \end{aligned} \quad (3.13)$$

with $x + L + iy = r_L e^{i\theta_L}$, $x - L + iy = r_R e^{i\theta_R}$ as usual and $f(r)$, $a(r)$ given in eq. (3.6), we can compute the energy as a function of φ . We choose a generic example with the couplings chosen as in fig. 2 and display the energy of the relative orientation rotated by U of eq. (3.12). The figure shows the energy during the flow towards the minimum of the energy functional while tracing the orientation φ , projected onto the $SO(2)$ subspace of $\mathbb{C}P^2$. The angle φ is not monotonic, but this is due to projecting onto the real subspace $SO(2)$. Regardless of the projection chosen, the end result is that the vortices align their moduli to point in the same direction. Notice, however, that they point in the same direction, but are not pointing in the 11 direction due to the midpoint between 11 and 22 being some off-diagonal point.

4 Conclusion and outlook

In this paper, we have studied non-Abelian vortices in the CFL phase in dense 3-flavor QCD in a non-axially symmetric setting, especially searching for molecule-like or spatially nontrivial configurations with one vortex in the left condensation and one in the right condensation. The chiral vortices can be rotated around in $\mathbb{C}P^2$ and by studying the system with a left and a right vortex, this potentially leads to quite a large space of initial conditions. We have found, however, that the vortex moduli attract and the minimizers of the energy functional that we found were always in the parallel state, i.e. both the left and the right vortex pointing in the same direction inside $\mathbb{C}P^2$. Exploring the parameter space, we have found characteristic examples of bound states of left and right vortices, that break the axial symmetry and finally we have found the most molecular-like state of two chiral

vortices on a chiral domain wall with two walls attached to each of the vortices – one of them binding the bound state and the other two ends tending off to infinity.

It would be interesting to get a better understanding of the vortex interactions in this model, which is quite complicated – especially at the nonlinear level, where the entire 9-dimensional parameter space kicks in. At the linear level, only the mass term and the Josephson term is probed by the scalar fields, but care must be taken for the non-Abelian gauge field to provide accurate predictions for the vortex interactions, which could probably be done by elaborating on the methods developed in ref. [76].

Non-axisymmetric vortex configurations found in this paper break the axial symmetry spontaneously, yielding a rotational Nambu-Goldstone mode. Such a mode, called a twiston, can propagate along the vortex line, as a helium-3 superfluid. The transition between axisymmetric and non-axisymmetric configurations may affect thermal properties of a vortex lattice, which could be relevant for the core of neutron stars. Another direction is a possible construction of a non-Abelian vorton, i.e. a closed vortex string with a non-trivial twist.

In this paper, electromagnetic interactions are neglected for simplicity. They can be taken into account in the presence of a non-Abelian vortex, resulting in a nontrivial potential on the CP^2 moduli [77] as well as an Aharonov-Bohm (AB) phase [78]. The vortex molecules in this paper also ought to be studied in the presence of electromagnetic interactions. The scattering of charged particles such as electrons and charged CFL pions off of a vortex should exhibit nontrivial AB phases. In addition to the electromagnetic AB phase, single chiral non-Abelian vortices exhibit non-Abelian AB phases, i.e. when (quasi-)quarks encircle the vortex it picks up color nonsinglet AB phases [63], similarly to the case of non-Abelian Alice strings in the 2SC + dd phase [79, 80], which are also confined into a single non-Abelian vortex [81]. The chiral non-Abelian vortex molecule may exhibit non-Abelian scattering if quarks can pass through between the two chiral vortices. One of the related nontrivial non-Abelian properties is the so-called topological obstruction, implying that generators of the unbroken symmetry in the ground state are not globally defined around the vortices [63]. This might be relevant for the topological properties of the ground state(s).

Finally, beyond the GL effective theory, it can be shown in the Bogoliubov-de Gennes equation, describing (quasi-)quark degrees of freedom, that an axisymmetric non-Abelian vortex admits three Majorana fermion zeromodes in its core [32–34]. Such Majorana fermion zeromodes turn non-Abelian vortices into non-Abelian anyons [82–84].

Acknowledgments

S. B. G. thanks the Outstanding Talent Program of Henan University for partial support. The work of M. N. is supported in part by JSPS KAKENHI [Grants No. JP22H01221] and the WPI program “Sustainability with Knotted Chiral Meta Matter (SKCM2)” at Hiroshima University (M. N.).

References

- [1] M. G. Alford, A. Schmitt, K. Rajagopal, and T. Schäfer, *Color superconductivity in dense quark matter*, *Rev. Mod. Phys.* **80** (2008) 1455–1515, [[arXiv:0709.4635](#)].
- [2] M. G. Alford, K. Rajagopal, and F. Wilczek, *Color flavor locking and chiral symmetry breaking in high density QCD*, *Nucl. Phys. B* **537** (1999) 443–458, [[hep-ph/9804403](#)].
- [3] M. G. Alford, K. Rajagopal, and F. Wilczek, *QCD at finite baryon density: Nucleon droplets and color superconductivity*, *Phys. Lett. B* **422** (1998) 247–256, [[hep-ph/9711395](#)].
- [4] R. Rapp, T. Schäfer, E. V. Shuryak, and M. Velkovsky, *Diquark Bose condensates in high density matter and instantons*, *Phys. Rev. Lett.* **81** (1998) 53–56, [[hep-ph/9711396](#)].
- [5] M. Eto, Y. Hirono, M. Nitta, and S. Yasui, *Vortices and Other Topological Solitons in Dense Quark Matter*, *PTEP* **2014** (2014), no. 1 012D01, [[arXiv:1308.1535](#)].
- [6] A. Balachandran, S. Digal, and T. Matsuura, *Semi-superfluid strings in high density QCD*, *Phys. Rev. D* **73** (2006) 074009, [[hep-ph/0509276](#)].
- [7] E. Nakano, M. Nitta, and T. Matsuura, *Non-Abelian strings in high density QCD: Zero modes and interactions*, *Phys. Rev. D* **78** (2008) 045002, [[arXiv:0708.4096](#)].
- [8] E. Nakano, M. Nitta, and T. Matsuura, *Non-Abelian Strings in Hot or Dense QCD*, *Prog. Theor. Phys. Suppl.* **174** (2008) 254–257, [[arXiv:0805.4539](#)].
- [9] M. Eto and M. Nitta, *Color Magnetic Flux Tubes in Dense QCD*, *Phys. Rev. D* **80** (2009) 125007, [[arXiv:0907.1278](#)].
- [10] M. Eto, E. Nakano, and M. Nitta, *Effective world-sheet theory of color magnetic flux tubes in dense QCD*, *Phys. Rev. D* **80** (2009) 125011, [[arXiv:0908.4470](#)].
- [11] M. Eto, M. Nitta, and N. Yamamoto, *Instabilities of Non-Abelian Vortices in Dense QCD*, *Phys. Rev. Lett.* **104** (2010) 161601, [[arXiv:0912.1352](#)].
- [12] A. Hanany and D. Tong, *Vortices, instantons and branes*, *JHEP* **07** (2003) 037, [[hep-th/0306150](#)].
- [13] R. Auzzi, S. Bolognesi, J. Evslin, K. Konishi, and A. Yung, *NonAbelian superconductors: Vortices and confinement in $N=2$ SQCD*, *Nucl. Phys. B* **673** (2003) 187–216, [[hep-th/0307287](#)].
- [14] A. Hanany and D. Tong, *Vortex strings and four-dimensional gauge dynamics*, *JHEP* **04** (2004) 066, [[hep-th/0403158](#)].
- [15] M. Shifman and A. Yung, *NonAbelian string junctions as confined monopoles*, *Phys. Rev. D* **70** (2004) 045004, [[hep-th/0403149](#)].
- [16] M. Eto, Y. Isozumi, M. Nitta, K. Ohashi, and N. Sakai, *Instantons in the Higgs phase*, *Phys. Rev. D* **72** (2005) 025011, [[hep-th/0412048](#)].
- [17] M. Eto, Y. Isozumi, M. Nitta, K. Ohashi, and N. Sakai, *Moduli space of non-Abelian vortices*, *Phys. Rev. Lett.* **96** (2006) 161601, [[hep-th/0511088](#)].
- [18] D. Tong, *TASI lectures on solitons: Instantons, monopoles, vortices and kinks*, in *Theoretical Advanced Study Institute in Elementary Particle Physics: Many Dimensions of String Theory*, 6, 2005. [[hep-th/0509216](#)].
- [19] M. Eto, Y. Isozumi, M. Nitta, K. Ohashi, and N. Sakai, *Solitons in the Higgs phase: The Moduli matrix approach*, *J. Phys. A* **39** (2006) R315–R392, [[hep-th/0602170](#)].

- [20] M. Shifman and A. Yung, *Supersymmetric Solitons and How They Help Us Understand Non-Abelian Gauge Theories*, *Rev. Mod. Phys.* **79** (2007) 1139, [[hep-th/0703267](#)].
- [21] M. Shifman and A. Yung, *Supersymmetric solitons*. Cambridge Monographs on Mathematical Physics. Cambridge University Press, 5, 2009.
- [22] M. Eto, M. Kurachi, and M. Nitta, *Constraints on two Higgs doublet models from domain walls*, *Phys. Lett. B* **785** (2018) 447–453, [[arXiv:1803.04662](#)].
- [23] M. Eto, M. Kurachi, and M. Nitta, *Non-Abelian strings and domain walls in two Higgs doublet models*, *JHEP* **08** (2018) 195, [[arXiv:1805.07015](#)].
- [24] M. Eto, Y. Hamada, M. Kurachi, and M. Nitta, *Topological Nambu monopole in two Higgs doublet models*, *Phys. Lett. B* **802** (2020) 135220, [[arXiv:1904.09269](#)].
- [25] M. Eto, Y. Hamada, M. Kurachi, and M. Nitta, *Dynamics of Nambu monopole in two Higgs doublet models. Cosmological Monopole Collider*, *JHEP* **07** (2020) 004, [[arXiv:2003.08772](#)].
- [26] M. Eto, Y. Hamada, and M. Nitta, *Topological structure of a Nambu monopole in two-Higgs-doublet models: Fiber bundle, Dirac’s quantization, and a dyon*, *Phys. Rev. D* **102** (2020), no. 10 105018, [[arXiv:2007.15587](#)].
- [27] M. Eto, Y. Hamada, and M. Nitta, *Stable Z-strings with topological polarization in two Higgs doublet model*, *JHEP* **02** (2022) 099, [[arXiv:2111.13345](#)].
- [28] M. M. Forbes and A. R. Zhitnitsky, *Global strings in high density QCD*, *Phys. Rev. D* **65** (2002) 085009, [[hep-ph/0109173](#)].
- [29] K. Iida and G. Baym, *Superfluid phases of quark matter. 3. Supercurrents and vortices*, *Phys. Rev. D* **66** (2002) 014015, [[hep-ph/0204124](#)].
- [30] M. Cipriani, W. Vinci, and M. Nitta, *Colorful boojums at the interface of a color superconductor*, *Phys. Rev. D* **86** (2012) 121704, [[arXiv:1208.5704](#)].
- [31] M. G. Alford, S. Mallavarapu, T. Vachaspati, and A. Windisch, *Stability of superfluid vortices in dense quark matter*, *Phys. Rev. C* **93** (2016), no. 4 045801, [[arXiv:1601.04656](#)].
- [32] S. Yasui, K. Itakura, and M. Nitta, *Fermion structure of non-Abelian vortices in high density QCD*, *Phys. Rev. D* **81** (2010) 105003, [[arXiv:1001.3730](#)].
- [33] T. Fujiwara, T. Fukui, M. Nitta, and S. Yasui, *Index theorem and Majorana zero modes along a non-Abelian vortex in a color superconductor*, *Phys. Rev. D* **84** (2011) 076002, [[arXiv:1105.2115](#)].
- [34] C. Chatterjee, M. Cipriani, and M. Nitta, *Coupling between Majorana fermions and Nambu-Goldstone bosons inside a non-Abelian vortex in dense QCD*, *Phys. Rev. D* **93** (2016), no. 6 065046, [[arXiv:1602.01677](#)].
- [35] M. Kobayashi, E. Nakano, and M. Nitta, *Color Magnetism in Non-Abelian Vortex Matter*, *JHEP* **06** (2014) 130, [[arXiv:1311.2399](#)].
- [36] Y. Hirono and M. Nitta, *Anisotropic optical response of dense quark matter under rotation: Compact stars as cosmic polarizers*, *Phys. Rev. Lett.* **109** (2012) 062501, [[arXiv:1203.5059](#)].
- [37] M. G. Alford, G. Baym, K. Fukushima, T. Hatsuda, and M. Tachibana, *Continuity of vortices from the hadronic to the color-flavor locked phase in dense matter*, *Phys. Rev. D* **99** (2019), no. 3 036004, [[arXiv:1803.05115](#)].
- [38] C. Chatterjee, M. Nitta, and S. Yasui, *Quark-hadron continuity under rotation: Vortex continuity or boojum?*, *Phys. Rev. D* **99** (2019), no. 3 034001, [[arXiv:1806.09291](#)].

- [39] C. Chatterjee, M. Nitta, and S. Yasui, *Quark-Hadron Crossover with Vortices*, *JPS Conf. Proc.* **26** (2019) 024030, [[arXiv:1902.00156](#)].
- [40] A. Cherman, S. Sen, and L. G. Yaffe, *Anyonic particle-vortex statistics and the nature of dense quark matter*, *Phys. Rev. D* **100** (2019), no. 3 034015, [[arXiv:1808.04827](#)].
- [41] Y. Hirono and Y. Tanizaki, *Quark-Hadron Continuity beyond the Ginzburg-Landau Paradigm*, *Phys. Rev. Lett.* **122** (2019), no. 21 212001, [[arXiv:1811.10608](#)].
- [42] Y. Hirono and Y. Tanizaki, *Effective gauge theories of superfluidity with topological order*, *JHEP* **07** (2019) 062, [[arXiv:1904.08570](#)].
- [43] A. Cherman, T. Jacobson, S. Sen, and L. G. Yaffe, *Higgs-confinement phase transitions with fundamental representation matter*, *Phys. Rev. D* **102** (2020), no. 10 105021, [[arXiv:2007.08539](#)].
- [44] Y. Hayashi, *Higgs-Confinement Continuity and Matching of Aharonov-Bohm Phases*, *Phys. Rev. Lett.* **132** (2024), no. 22 221901, [[arXiv:2303.02129](#)].
- [45] A. Cherman, T. Jacobson, S. Sen, and L. G. Yaffe, *Line operators, vortex statistics, and Higgs versus confinement dynamics*, *JHEP* **06** (2024) 200, [[arXiv:2401.17489](#)].
- [46] T. Hayata, Y. Hidaka, and D. Kondo, *Phase transition on superfluid vortices in Higgs-Confinement crossover*, [arXiv:2411.03676](#).
- [47] E. Babaev, *Vortices carrying an arbitrary fraction of magnetic flux quantum in two gap superconductors*, *Phys. Rev. Lett.* **89** (2002) 067001, [[cond-mat/0111192](#)].
- [48] Y. Tanaka, *Phase instability in multi-band superconductors*, *Journal of the Physical Society of Japan* **70** (2001), no. 10 2844–2847.
- [49] Y. Tanaka, *Soliton in two-band superconductor*, *Phys. Rev. Lett.* **88** (Dec, 2001) 017002.
- [50] J. Goryo, S. Soma, and H. Matsukawa, *Deconfinement of vortices with continuously variable fractions of the unit flux quanta in two-gap superconductors*, *Europhysics Letters (EPL)* **80** (sep, 2007) 17002.
- [51] D. F. Agterberg, *Vortex lattice structures of Sr_2RuO_4* , *Phys. Rev. Lett.* **80** (Jun, 1998) 5184–5187.
- [52] J. Garaud and E. Babaev, *Skyrmionic state and stable half-quantum vortices in chiral p-wave superconductors*, *Phys. Rev. B* **86** (Aug, 2012) 060514.
- [53] D. T. Son and M. A. Stephanov, *Domain walls in two-component Bose-Einstein condensates*, *Phys. Rev. A* **65** (2002) 063621, [[cond-mat/0103451](#)].
- [54] K. Kasamatsu, M. Tsubota, and M. Ueda, *Vortex molecules in coherently coupled two-component Bose-Einstein condensates*, *Phys. Rev. Lett.* **93** (2004), no. 25 250406, [[cond-mat/0406150](#)].
- [55] M. Cipriani and M. Nitta, *Crossover between integer and fractional vortex lattices in coherently coupled two-component Bose-Einstein condensates*, *Phys. Rev. Lett.* **111** (2013) 170401, [[arXiv:1303.2592](#)].
- [56] M. Tylutki, L. P. Pitaevskii, A. Recati, and S. Stringari, *Confinement and precession of vortex pairs in coherently coupled Bose-Einstein condensates*, *Phys. Rev. A* **93** (2016), no. 4 043623, [[arXiv:1601.03695](#)].
- [57] M. Eto and M. Nitta, *Confinement of half-quantized vortices in coherently coupled Bose-Einstein condensates: Simulating quark confinement in a QCD-like theory*, *Phys. Rev.*

- A* **97** (2018), no. 2 023613, [[arXiv:1702.04892](#)].
- [58] M. Eto, K. Ikeno, and M. Nitta, *Collision dynamics and reactions of fractional vortex molecules in coherently coupled Bose-Einstein condensates*, *Phys. Rev. Res.* **2** (2020), no. 3 033373, [[arXiv:1912.09014](#)].
- [59] M. Kobayashi, M. Eto, and M. Nitta, *Berezinskii-Kosterlitz-Thouless Transition of Two-Component Bose Mixtures with Intercomponent Josephson Coupling*, *Phys. Rev. Lett.* **123** (2019), no. 7 075303, [[arXiv:1802.08763](#)].
- [60] C. Chatterjee, S. B. Gudnason, and M. Nitta, *Chemical bonds of two vortex species with a generalized Josephson term and arbitrary charges*, *JHEP* **04** (2020) 109, [[arXiv:1912.02685](#)].
- [61] M. Eto and M. Nitta, *Vortex trimer in three-component Bose-Einstein condensates*, *Phys. Rev. A* **85** (2012) 053645, [[arXiv:1201.0343](#)].
- [62] M. Eto and M. Nitta, *Vortex graphs as N -omers and $CP(N-1)$ Skyrmions in N -component Bose-Einstein condensates*, *EPL* **103** (2013), no. 6 60006, [[arXiv:1303.6048](#)].
- [63] M. Eto and M. Nitta, *Chiral non-Abelian vortices and their confinement in three flavor dense QCD*, *Phys. Rev. D* **104** (2021), no. 9 094052, [[arXiv:2103.13011](#)].
- [64] M. Eto, Y. Hirono, and M. Nitta, *Domain Walls and Vortices in Chiral Symmetry Breaking*, *PTEP* **2014** (2014), no. 3 033B01, [[arXiv:1309.4559](#)].
- [65] K. Iida and G. Baym, *The Superfluid phases of quark matter: Ginzburg-Landau theory and color neutrality*, *Phys. Rev. D* **63** (2001) 074018, [[hep-ph/0011229](#)]. [Erratum: *Phys.Rev.D* **66**, 059903 (2002)].
- [66] K. Iida and G. Baym, *Superfluid phases of quark matter. 2: phenomenology and sum rules*, *Phys. Rev. D* **65** (2002) 014022, [[hep-ph/0108149](#)].
- [67] I. Giannakis and H.-c. Ren, *The Ginzburg-Landau free energy functional of color superconductivity at weak coupling*, *Phys. Rev. D* **65** (2002) 054017, [[hep-ph/0108256](#)].
- [68] M. Nitta, *Non-Abelian Sine-Gordon Solitons*, *Nucl. Phys. B* **895** (2015) 288–302, [[arXiv:1412.8276](#)].
- [69] M. Eto and M. Nitta, *Non-Abelian Sine-Gordon Solitons: Correspondence between $SU(N)$ Skyrmions and CP^{N-1} Lumps*, *Phys. Rev. D* **91** (2015), no. 8 085044, [[arXiv:1501.07038](#)].
- [70] M. Eto, K. Nishimura, and M. Nitta, *Phases of rotating baryonic matter: non-Abelian chiral soliton lattices, antiferro-isospin chains, and ferri/ferromagnetic magnetization*, *JHEP* **08** (2022) 305, [[arXiv:2112.01381](#)].
- [71] M. Nitta, *Josephson junction of non-Abelian superconductors and non-Abelian Josephson vortices*, *Nucl. Phys. B* **899** (2015) 78–90, [[arXiv:1502.02525](#)].
- [72] M. Nitta, *Josephson instantons and Josephson monopoles in a non-Abelian Josephson junction*, *Phys. Rev. D* **92** (2015), no. 4 045010, [[arXiv:1503.02060](#)].
- [73] M. Nitta, *Relations among topological solitons*, *Phys. Rev. D* **105** (2022), no. 10 105006, [[arXiv:2202.03929](#)].
- [74] M. Eto, K. Nishimura, and M. Nitta, *Domain-wall Skyrmion phase in a rapidly rotating QCD matter*, *JHEP* **03** (2024) 019, [[arXiv:2310.17511](#)].
- [75] Y. Amari and M. Nitta, *Skyrmion crystal phase on a magnetic domain wall in chiral magnets*, [[arXiv:2409.07943](#)].
- [76] J. M. Speight, *Static intervortex forces*, *Phys. Rev. D* **55** (1997) 3830–3835,

- [hep-th/9603155].
- [77] W. Vinci, M. Cipriani, and M. Nitta, *Spontaneous Magnetization through Non-Abelian Vortex Formation in Rotating Dense Quark Matter*, *Phys. Rev. D* **86** (2012) 085018, [[arXiv:1206.3535](#)].
- [78] C. Chatterjee and M. Nitta, *Aharonov-Bohm Phase in High Density Quark Matter*, *Phys. Rev. D* **93** (2016), no. 6 065050, [[arXiv:1512.06603](#)].
- [79] Y. Fujimoto and M. Nitta, *Non-Abelian Alice strings in two-flavor dense QCD*, *Phys. Rev. D* **103** (2021) 054002, [[arXiv:2011.09947](#)].
- [80] Y. Fujimoto and M. Nitta, *Alice meets Boojums in neutron stars: vortices penetrating two-flavor quark-hadron continuity*, *Phys. Rev. D* **103** (2021), no. 11 114003, [[arXiv:2102.12928](#)].
- [81] Y. Fujimoto and M. Nitta, *Topological confinement of vortices in two-flavor dense QCD*, *JHEP* **09** (2021) 192, [[arXiv:2103.15185](#)].
- [82] S. Yasui, K. Itakura, and M. Nitta, *Majorana meets Coxeter: Non-Abelian Majorana Fermions and Non-Abelian Statistics*, *Phys. Rev. B* **83** (2011) 134518, [[arXiv:1010.3331](#)].
- [83] Y. Hirono, S. Yasui, K. Itakura, and M. Nitta, *Non-Abelian statistics of vortices with multiple Majorana fermions*, *Phys. Rev. B* **86** (2012) 014508, [[arXiv:1203.0173](#)].
- [84] Y. Masaki, T. Mizushima, and M. Nitta, *Non-Abelian Anyons and Non-Abelian Vortices in Topological Superconductors*, *Encyclopedia of Condensed Matter Physics (Second Edition)* **2** (1, 2024) 755–794, [[arXiv:2301.11614](#)].